Synchronization of pulse-coupled oscillators with a refractory period and frequency distribution for a wireless sensor network

Synchronization of pulse-coupled oscillators with a refractory period and frequency distribution for a wireless sensor network

Keiji Konishi* and Hideki Kokame

Dept. of Electrical and Information Systems, Osaka Prefecture University

1-1 Gakuen-cho, Naka-ku, Sakai, Osaka, 599-8531 Japan

(Dated: July 9, 2008)

Abstract

The present paper considers the synchronization of globally pulse-coupled oscillators with a refractory period and frequency distribution. The oscillators are capable of achieving time synchronization for a practical wireless sensor network. Furthermore, as a result of the stability analysis of the synchronization, a procedure for designing the oscillators is provided: the determination of the allowable refractory period under a given frequency distribution range. These analytical results are verified by numerical examples.

*URL: http://www.eis.osakafu-u.ac.jp

Lead Paragraph

The present paper considers the synchronization of globally pulse-coupled oscillators with a refractory period and frequency distribution. The time synchronization of the oscillators is important for a practical wireless sensor network. This is because the time synchronization is needed for various sensor fusion applications and plays an important role in coordinating communication among nodes. The main result of this paper provides a simple systematic procedure for designing the oscillators: the determination of the allowable refractory period under a given frequency distribution range. The result is useful not only for physics but also for information and computer engineering.

I. INTRODUCTION

Synchronization in coupled nonlinear oscillators have been investigated over the years not only in the field of electrical engineering [1–3], but also in nonlinear physics for the purposes of clarifying the mechanism of complex phenomena in nature [4, 5]. Among these coupled oscillators, a pulse-coupled network, which consists of integrate-fire oscillators interacting with each other by impulse signals, has been used as a prototype model for the synchronization of biological oscillators including the pacemaker cells of the heart. Mirollo and Strogatz reported that a global (i.e., all to all) pulse-coupled network exhibits synchronization for almost all initial conditions [6]. This type of network has been further extended and investigated for practical situations: inhomogeneous oscillators with a frequency distribution [7, 8], effects of adding a refractory period to all of the oscillators [9, 10], transmission delay of the pulse signals [11–14], a local coupled network [8, 12, 15–17], and various network topologies [18]. Furthermore, synchronization was experimentally observed in a pulse-coupled network implemented by simple electronic circuits [19–24].

In recent years, wireless sensor networks have been intensively studied in the field of information and computer science [25]. Figure 1 illustrates a wireless sensor network and a node structure. This network consists of spatially distributed autonomous sensor nodes: each node communicates with the other nodes and monitors physical values such as temperature, sound, and pressure. Each node has sensor devices, computation capability (e.g., computer), a communication device (e.g., a transmitter (TX) and a receiver (RX)), and a power supply (e.g., battery). Wireless sensor networks are now expected to be used for a wide variety of applications. However, there are still several technical problems to be worked out. A crucial problem is that each sensor node must have access

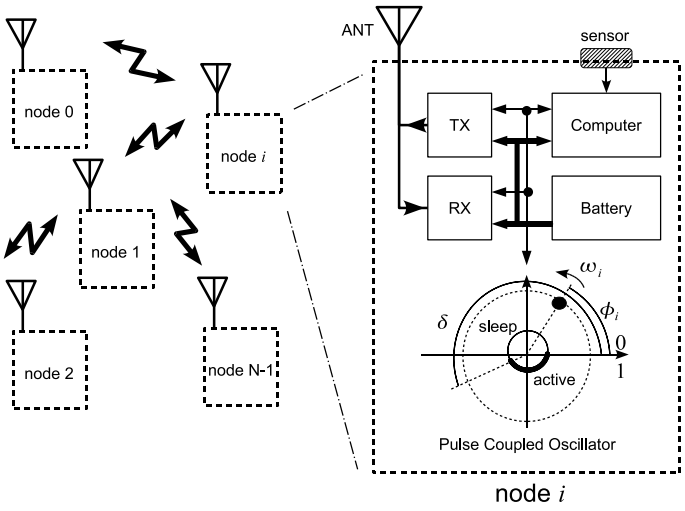

FIG. 1: Illustration of a wireless sensor network and node structure.

to an accurate internal clock. In other words, their clocks should be accurately synchronized for two reasons: time synchronization is needed for various sensor fusion applications and the synchronization plays an important role in coordinating communication among nodes [26]. Thus, the time synchronization problem becomes recognized as one of the crucial problems for a wireless sensor network. **Many researchers have proposed the various rules (i.e., protocols) governing synchronization in order to overcome this problem [26]. However, these protocols often require the computation of message exchange and processing, which wastes the limited computation capability of nodes and causes communication delays. On the other hand, a pulse-coupled oscillators (PCOs) synchronization strategy [27–33] does not require such computation, since the PCOs broadcasting pulse signals instead of packet message can be implemented by hardware at the physical layer of the OSI reference model [33].**

For wireless sensor networks, it is often assumed that a lot of tiny sensor nodes are spatially distributed and the number of nodes changes from hour to hour. Accordingly, the following three problems must be considered. First, the autonomous nodes should save electric power to increase the life of its battery, since they do not have an external electronic power-supply. Second, in order to reduce hardware costs, the nodes have to use standard popular-priced electronic devices, which are not high precision. Finally, the time synchronization should be robust even if the number of nodes changes.

The present paper considers globally pulse-coupled oscillators that can overcome the above

three problems. The oscillators are assumed to have the following characteristics: all the oscillators have a long refractory period during which the receiver sleeps to cut power consumption; there are variations in the oscillators' frequency due to the popular-priced electronic devices; synchronization is maintained even when nodes are deleted or added. The main purposes of this paper are to analyze the dynamics of the pulse-coupled oscillators and to provide a systematic procedure for designing the refractory period, on the basis of a given variation range of the oscillators' frequency, both for minimizing the electronic power consumption and maintaining the synchronization. To verify the proposed procedure, some numerical examples are presented.

II. PULSE-COUPLED OSCILLATORS

Consider a network of N oscillators (i.e., N nodes). The phase of i-th oscillator, denoted by $\phi_i(t) \in [0, 1]$, envelopes with parameter $\omega_i \in [\underline{\omega}, 1]$; that is,

$$\frac{\mathrm{d}\phi_i(t)}{\mathrm{d}t} = \omega_i, \quad (i = 0, 1, \ldots, N-1). \tag{1}$$

For the sake of simplicity, the upper limit of ω_i is normalized as 1, and then the lower limit is set to $\underline{\omega}$. Thus the parameter is in the range: $\omega_i \in [\underline{\omega}, 1]$. **Let $k \in \boldsymbol{Z}_+$ be the number of firings in the network. When the phase $\phi_i(t)$ reaches 1 at time t^{k-}, the i-th oscillator fires and broadcasts an impulse signal to all the other oscillators. Then, it is immediately reset to zero at t^{k+},**

$$\phi_i(t^{k-}) = 1 \;\Rightarrow\; \phi_i(t^{k+}) = 0. \tag{2}$$

At the same time, the other oscillators being active, $\phi_j(t^{k-}) \in [\delta, 1)$ (i.e., receiver works), are forced to be reset to zero by the broadcast impulse signal:

$$\phi_i(t^{k-}) = 1 \text{ and } \phi_j(t^{k-}) \in [\delta, 1) \;\Rightarrow\; \phi_j(t^{k+}) = 0 \;\; \forall j \neq i. \tag{3}$$

On the contrary, the sleeping oscillators, $\phi_j(t^{k-}) \in (0, \delta)$ (i.e., receiver sleeps), are not reset:

$$\phi_i(t^{k-}) = 1 \text{ and } \phi_j(t^{k-}) \in (0, \delta) \;\Rightarrow\; \phi_j(t^{k+}) = \phi_j(t^{k-}) \;\; \forall j \neq i. \tag{4}$$

It is obvious that the time interval of the receiver being active, $[\delta, 1)$, becomes shorter as δ increases. The mathematical description of the network dynamics, which can be described by a nonlinear discrete-time map, is given in Appendix.

Now the relationship between the oscillators proposed in the present paper and the original oscillators proposed by Mirollo and Strogatz [6] is clarified. The present oscillators have the following four features compared with the original: the function $x = f(\phi)$, which describes the relationship between the system state x and the phase ϕ, is simplified as a linear function, $f(\phi) := \phi$; the firing strength is set to infinity; the parameter values, ω_i, are distributed; the active and sleep periods are introduced. The first and second features specialize the original oscillators; on the contrary, the others extend the original specification. **The third feature has already been introduced in the field of physics [7, 8] and networks [30]; furthermore, the fourth has also been investigated in that of physics [9, 10] and networks [33].** Very few works have been found to be currently available on both of third and fourth features. Nevertheless, as mentioned in the previous section, for sensor networks, it is important to consider oscillators that have both of the features.

The main concrete purpose of this paper is to solve a design problem. The problem has three assumptions: the parameters ω_i are unknown, but the lower limit $\underline{\omega}$ is known; the initial conditions of all oscillators are completely unknown; the number of oscillators, N, is unknown and several oscillators are added or deleted at some time. These are reasonable assumptions for practical sensor networks. First, an integrate-and-fire oscillator was experimentally realized by charging and discharging a capacitor [19–22]. In this case, the capacitance accuracy is proportional to the oscillator frequency accuracy. In general, popular-priced capacitors are not highly-accurate, but their maximum error (e.g., $\pm 10\%$) can be obtained from their data sheet. This situation explains the first assumption. Second, the initial condition of the oscillators corresponds to the initial electric charge of the capacitances. It can be easily understood that it is not practical to check the initial electric charge of all of the oscillators. The second assumption represents this situation. Third, it is natural that some of the numerous sensor nodes break down and new nodes are added to replace the broken nodes. The third assumption represents this situation.

Under these assumptions, the present paper tries to design a refractory period δ such that: the oscillators should be synchronized at most a given n fires after new nodes are added; δ is maximized. These two specifications are required for practical reasons. The first specification guarantees that the recovery period from a disturbance (e.g., new nodes added) is equal or less n. This period represents a crucial performance, or robustness, of the networks. The second specification indicates that in order to cut power consumption, the refractory period should be extended as long as possible.

III. DEFINITIONS OF STABILITY

In this section, the definitions of synchronization and two types of stability of synchronization in the network described by (1), (2), (3), (4) are provided. Before the definitions, the maximum frequency of all the oscillators is denoted by

$$\hat{\omega} := \max_{i \in \{0,1,\ldots,N-1\}} \omega_i. \tag{5}$$

First, a definition of synchronization is introduced.

[**Synchronization**] All the oscillators are said to **synchronize** if they repeat to fire simultaneously,

$$\phi_i(t^{k+}) = 0,\ \forall i \in \{0, 1, \ldots, N-1\},\ \forall k \geq n, \tag{6}$$

with a constant period,

$$t^{(k+1)+} - t^{k+} = \frac{1}{\hat{\omega}},\ \forall k \geq n, \tag{7}$$

after n fires.

Second, two definitions of stability of synchronization are detailed.

[**Local stability**] Suppose that the initial condition of every oscillator is

$$\phi_i(0) \in [\delta, 1],\ \forall i \in \{0, 1, \ldots, N-1\}. \tag{8}$$

The synchronization is said to be **locally stable** if all the oscillators have been synchronized since the first fire ($n = 1$).

[**Global stability**] Suppose that the initial condition of every oscillator is

$$\phi_i(0) \in [0, 1],\ \forall i \in \{0, 1, \ldots, N-1\}. \tag{9}$$

The synchronization is said to be **globally stable** if all the oscillators have been synchronized since the n-th fire.

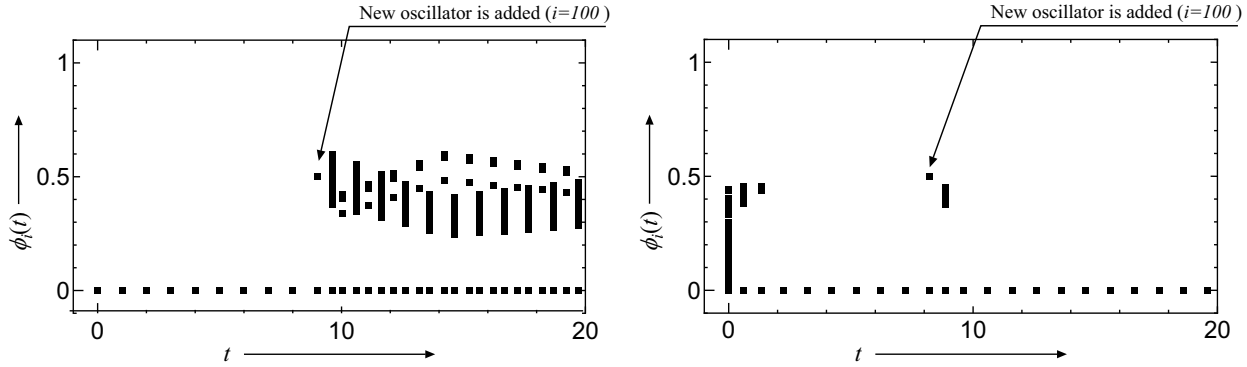

(a) $\delta = 0.600$, $0.7 < \phi_i(0) < 1.0$ (b) $\delta = 0.457$, $0.0 < \phi_i(0) < 1.0$

FIG. 2: Stroboscopic view on the phase $\phi_i(t)$ of $N = 100$ at each fire time t^{k+} ($\underline{\omega} = 0.60$). Just after the 10th fire, a new node with $\phi_{100}(t^{10+}) = 0.5$ and $\omega_{100} = 0.8$ is added to the network.

Since initial condition (8) is included in condition (9), it is noticed that global stability possesses local stability. However, in this paper, the concept of local stability cannot be used to design the oscillators due to the second and third assumptions. Thus, global stability is primarily used to design the oscillators.

In order to grasp the difference between local and global stability, numerical examples are presented. Figure 2 plots a stroboscopic view on the phase $\phi_i(t)$ of $N = 100$ at each fire time t^{k+}. The differences between Figs. 2(a) and 2(b) are the refractory period δ and initial conditions; the other parameters are the same. Just after the 10th fire, a new oscillator with $\phi_{100}(t^{10+}) = 0.5$ and $\omega_{100} = 0.8$ is added to the network. In Fig. 2(a), the initial condition satisfies condition (8), so the oscillators synchronize from the first fire to the 10th fire. After the addition of a new oscillator, the synchronization breaks down. This result indicates that the synchronization is locally stable. In Fig. 2(b), the initial conditions are distributed on the range (9), then the oscillators synchronize from the 4th to the 10th fires. After the addition of a new oscillator, the synchronization temporarily breaks down, but recovers within two fires. Hence, Fig. 2(b) shows that the synchronization is globally stable.

IV. STABILITY ANALYSIS

In this section, a solution to the problem of how to design a refractory period δ that guarantees the local and global stability of the synchronization is provided.

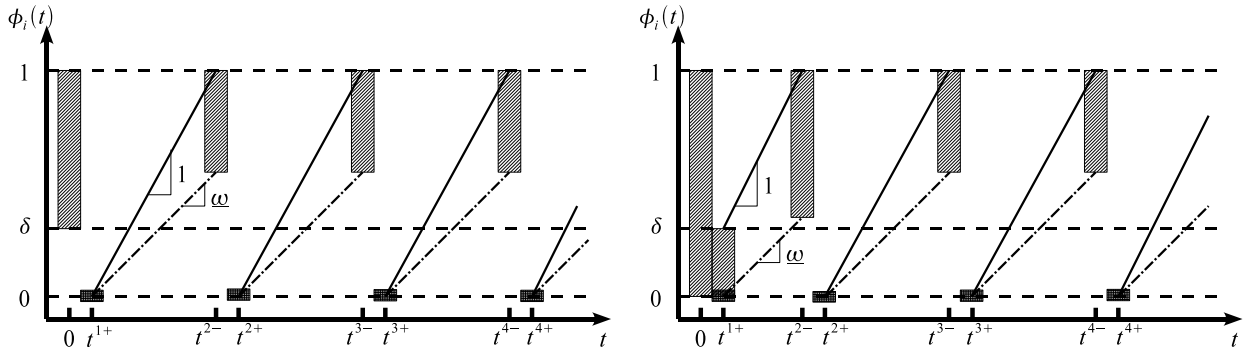

(a) Local stable (b) Global stable

FIG. 3: Illustration of phase distribution at just before and after fire times $t^{k\pm}$.

A. Local stability condition

First, local stability is considered. Figure 3(a) illustrates the phase $\phi_i(t)$ with local stability at just before and after fire times $t^{k\pm}$. The phases are within the shaded regions at $t^{k\pm}$. The initial condition is given by condition (8). Since all the oscillators are in the active region at $t = 0$, an oscillator's fire induces the other oscillators' fire. This fire causes all the oscillators to be reset to zero at t^{1+}. After that, the phase $\phi_i(t)$ is increased at the rate ω_i, where the upper and lower bounds of the increasing rate are 1 (solid line) and $\underline{\omega}$ (dashed-dotted line). As the upper and lower bounds are 1 and $\underline{\omega}$, $t^{2+} - t^{1+} \geq 1$ and $t^{2+} - t^{1+} \leq 1/\underline{\omega}$ are provided. The phase distribution at just before the second fire is limited to a subinterval $[\underline{\omega}, 1]$. Hence, if $\underline{\omega} \geq \delta$ is held, all the oscillators are reset to zero at t^{2+}. Since the same firing sequence is repeated after the second fire, the synchronization is eternally maintained. From the above discussion, a sufficient condition for the local stability is as follows.

[Local stability condition] If the lower bound of the parameter, $\underline{\omega}$, is greater than or equal to the refractory period δ,

$$\delta \leq \underline{\omega}, \tag{10}$$

then the synchronization is locally stable.

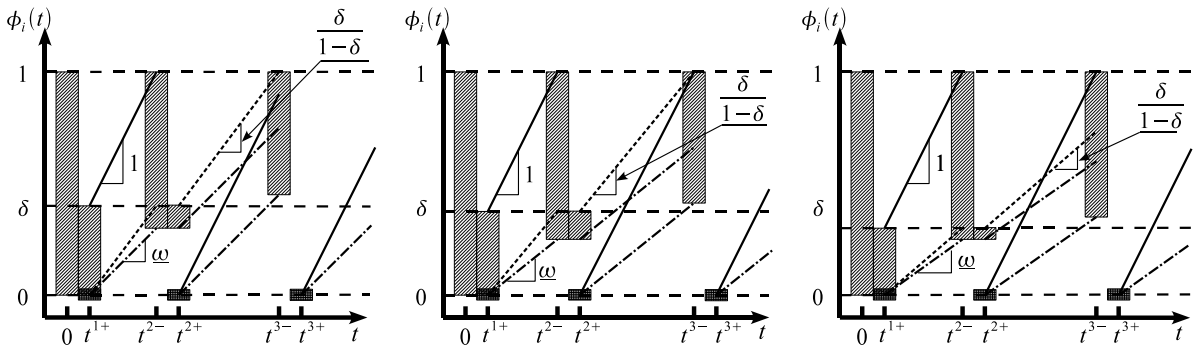

(a) $\delta > \delta_3^*$ (b) $\delta = \delta_3^*$ (c) $\delta < \delta_3^*$

FIG. 4: Illustration of phase distribution at just before and after fire times $t^{k\pm}$. The synchronization is globally stable ($n = 3$).

B. Global stability condition

Next, global stability is considered. Figure 3(b) illustrates the phases $\phi_i(t)$ having global stability at just before and after fire times $t^{k\pm}$. The initial state is given by condition (9). Just after the first fire, t^{1+}, the phases within the active region are reset to zero, but the phases outside the region (i.e., within the sleep region) remain unchanged. After t^{1+}, the phases $\phi_i(t)$ are increased at the rate ω_i. The upper and lower bounds of the increasing rate are 1 (solid line) and $\underline{\omega}$ (dashed-dotted line). The earliest possible time for the second fire is estimated to be $t^{2-} = t^{1+} + 1 - \delta$. The phase distribution at t^{2-} is given by $\phi_i(t^{2-}) \in [\underline{\omega}(1-\delta), 1]$. Consequently, if the distribution at t^{2-} is within the active region, that is,

$$\delta \leq \underline{\omega}(1-\delta) \Leftrightarrow \delta \leq \frac{\underline{\omega}}{1+\underline{\omega}}, \tag{11}$$

then all the oscillators fire at t^{2-}, and then are reset to zero at t^{2+}. If condition (11) is satisfied, the synchronization is maintained after that point.

Now the case in which the oscillators synchronize after at most three fires, $\underline{\omega} < \delta$, is considered as shown in Fig. 4. For $t \in [0, t^{2-}]$, the same behavior as in Fig. 3(b) is evident. However, just after the second fire, t^{2+}, the phases within the active region are reset to zero as shown in Fig. 4. After t^{2+} they increase within the upper (solid line with slope 1) and lower (dashed-dotted line with slope $\underline{\omega}$) bounds. On the other hand, the phases outside the region at t^{2-} still remain; after t^{2+} they increase within the upper (dashed line with slope $\delta/(1-\delta)$) and lower (dashed-dotted line with slope $\underline{\omega}$) bounds. The upper bound rate, $\delta/(1-\delta)$, is the largest possible rate ω_i of the oscillators unfired at t^{2-}. It is noticed that the third fire can be classified into the three cases

sketched in Fig. 4: Figure 4(a) (4(c)) illustrates the case in which the oscillators unfired (fired) at t^{2-} lead to the third fire; the marginal case is sketched in Fig. 4(b). From these sketches, it is easily seen that the marginal case occurs for $\delta = \delta_3^*$, where $\delta_3^* := (1-\delta_3^*)^2,\ \delta_3^* \in (0,1)$. Thus, the time interval between the second and third fires is

$$t^{3-} - t^{2-} \geq \begin{cases} (1-\delta)^2/\delta & \text{if} \quad \delta \geq \delta_3^* \\ 1 & \text{if} \quad \delta \leq \delta_3^* \end{cases}. \tag{12}$$

The lower bound slope $\underline{\omega}$ in Fig. 4 (dashed-dotted line) guarantees that the smallest phase at t^{3-} satisfies

$$\min_{i\in\{0,1....,N-1\}} \phi_i(t^{3-}) \geq \underline{\omega}(t^{3-} - t^{2-}). \tag{13}$$

On the other hand, it is obvious that if

$$\min_{i\in\{0,1....,N-1\}} \phi_i(t^{3-}) \geq \delta \tag{14}$$

holds, then all the oscillators synchronize after at most three fires. Thus, condition (13) allows the sufficient condition of (14) to be obtained, which is described by

$$\underline{\omega}(t^{3-} - t^{2-}) \geq \delta. \tag{15}$$

As a consequence, it can be said that, if condition (15) is held, then all the oscillators synchronize after at most three fires. Substituting inequality (12) into condition (15) yields

$$\delta \leq \begin{cases} \dfrac{\sqrt{\underline{\omega}}}{1+\sqrt{\underline{\omega}}} & \text{if} \quad \delta \geq \delta_3^* \\ \underline{\omega} & \text{if} \quad \delta \leq \delta_3^* \end{cases}. \tag{16}$$

This condition is equivalent to

$$\delta \leq \begin{cases} \dfrac{\sqrt{\underline{\omega}}}{1+\sqrt{\underline{\omega}}} & \text{if} \quad \underline{\omega} \geq \omega_3^* \\ \underline{\omega} & \text{if} \quad \underline{\omega} \leq \omega_3^* \end{cases}, \tag{17}$$

where ω_3^* is a solution of $\omega = (1-\omega)^2$, $\omega \in (0,1)$.

The above discussion is now generalized. Figure 5 illustrates the phase distribution synchronized after at most n fires. The fire pattern in which the unfired oscillators lead to the next fire (see Fig. 4(a)) is repeated until the $(n-1)$th fire. The three cases mentioned in Fig. 4, that is $\delta >, =, < \delta_3^*$, are also valid for any number of fires; Figure 4 corresponds to Fig. 5 with the exception of the

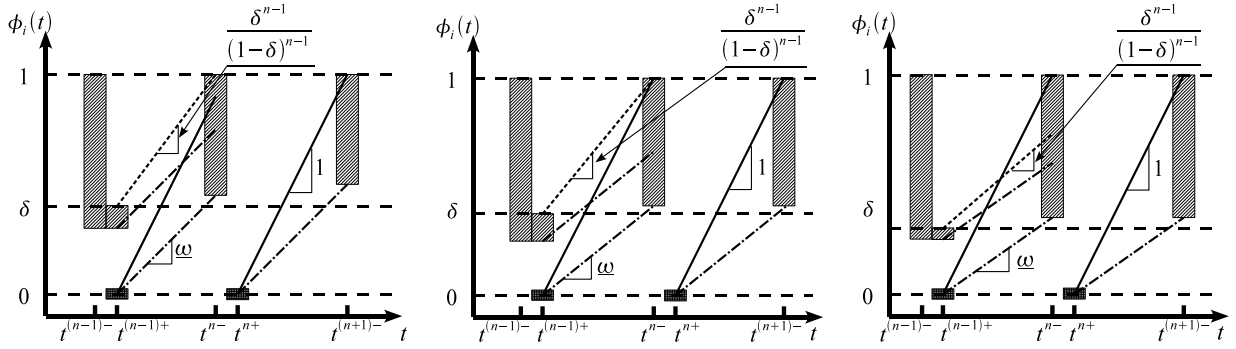

(a) $\delta > \delta_n^*$ (b) $\delta = \delta_n^*$ (c) $\delta < \delta_n^*$

FIG. 5: Illustration of phase distribution at just before and after fire times $t^{t\pm}$. The synchronization is globally stable (n).

slopes. The phases fired at $t^{(n-1)-}$ increase within the upper (solid line with slope 1) and lower (dashed-dotted line with slope $\underline{\omega}$) bounds. On the other hand, the phases that remain unfired at $t^{(n-1)-}$ increase within the upper (dashed line with slope $\delta^{n-1}/(1-\delta)^{n-1}$) and lower (dashed-dotted line with slope $\underline{\omega}$) bounds. In a similar way to the $n = 3$ case, the following condition can be obtained.

[Global stability condition] If the lower bound of the parameter, $\underline{\omega}$, and the refractory period δ satisfy

$$\delta \leq g(n, \underline{\omega}), \tag{18}$$

$$g(n, \underline{\omega}) := \begin{cases} \dfrac{\sqrt[n-1]{\underline{\omega}}}{1 + \sqrt[n-1]{\underline{\omega}}} & \text{if} \quad \underline{\omega} \geq \omega_n^* \\ \underline{\omega} & \text{if} \quad \underline{\omega} \leq \omega_n^* \end{cases}, \tag{19}$$

$$\omega_n^* := \left\{ \omega : \omega \in [0, 1),\ (1-\omega)^{n-1} = \omega^{n-2} \right\}, \tag{20}$$

then all the oscillators synchronize after at most $n(\geq 2)$ fires for any initial condition.

These analytical results shall be confirmed by numerical simulations in the next section.

V. NUMERICAL SIMULATIONS AND DISCUSSIONS

This section shall confirm the analytical results by numerical simulations, and discuss the procedure for designing the oscillators.

A. Numerical simulations

The number of fires needed to achieve synchronization for $\delta \in (0, 1)$ and $\underline{\omega} \in (0, 1)$ is checked. The number of oscillators is set to $N = 500$, and their initial phases are randomly chosen from Eq. (9). The oscillators with a fixed parameter set $\{\delta, \underline{\omega}\}$ runs until $t = 100$. This run is repeated 20 times, and then the maximum number of fires is recorded. As shown in Fig. 6(a), the recorded number represented by

2: red, 3: blue, 4: green

is plotted for $\delta \in (0, 1)$ and $\underline{\omega} \in (0, 1)$. In addition, the function $g(n, \underline{\omega})$ in Eq. (19) is represented by the solid lines. As predicted, the global stability condition derived in the previous section guarantees that the oscillators synchronize after at most n fires for the parameter set under the solid line $g(n, \underline{\omega})$. It can be seen that the blue dots ($n = 3$) are not plotted under $g(2, \underline{\omega})$; further, a similar fact is also observed for $g(3, \underline{\omega})$. Figure 6(b) is the expansion of the rectangular area enclosed by the dashed lines in Fig. 6(a). As can be seen from the figure, a similar trend is observed for $g(4, \underline{\omega})$, $g(5, \underline{\omega})$, and $g(6, \underline{\omega})$. The parameter set represented by point A in Fig. 6(a) satisfies the local stability condition, but does not satisfy the global condition. The phase distribution at point A is shown in Fig. 2(a). Furthermore, point B in Fig. 6(b) satisfies the global condition. The phase distribution at point B is shown in Fig. 2(b). These numerical simulations entirely agree with the stability condition.

B. Systematic procedure for designing oscillators

Now the design problem described in Sec. II can be solved. The problem is to design the refractory period δ to satisfy the two specifications under the three assumptions. From the global stability condition derived in Sec. IV, the period $\delta = g(n, \underline{\omega})$ can be determined. This is a solution to the problem.

The design procedure is now followed using a numerical example. For the first assumption, the lower bound of the parameter is known as $\underline{\omega} = 0.6$. For the second assumption, the initial phases

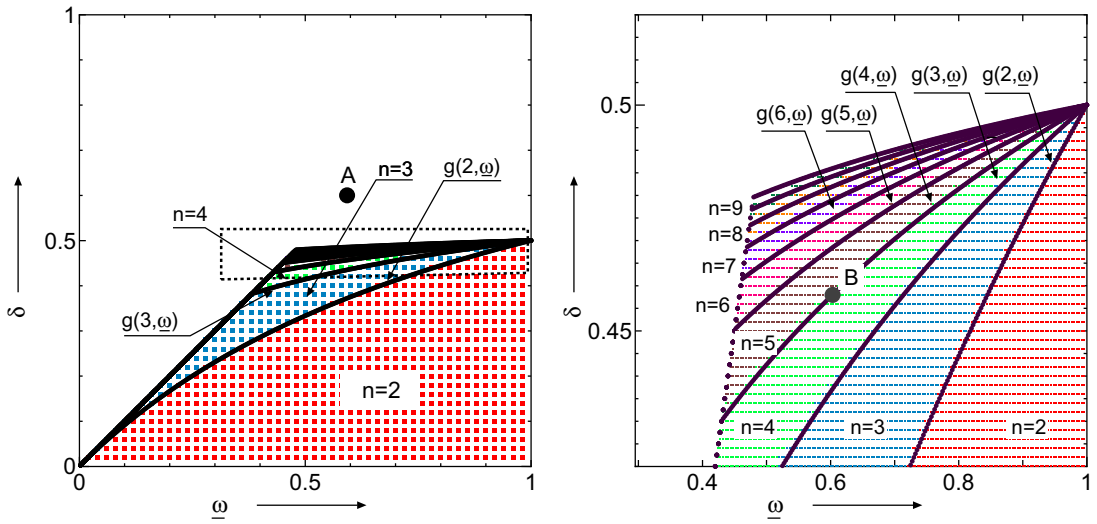

(a) $\underline{\omega} \in (0.0, 1.0)$, $\delta \in (0.0, 1.0)$ (b) $\underline{\omega} \in (0.3, 1.0)$, $\delta \in (0.3, 0.6)$

FIG. 6: Maximum number of fires to achieve the synchronization for $\delta \in (0, 1)$ and $\underline{\omega} \in (0, 1)$.

are randomly chosen from $\phi_i(0) \in [0, 1]$, but their values are unknown. For the third assumption, the number of oscillators is set to $N = 100$ and new oscillators are added to the network at t^{10+}, but the number of oscillators and information concerning the addition are unknown. For the first specification, the oscillators should be synchronized after at most four fires after the new oscillators are added. For the second specification, δ is maximized. According to the global stability condition, $\delta = g(4, 0.6) = 0.457$ is designed, which represents point B in Fig. 6(b). The phase distribution of the designed oscillators is shown in Fig. 2(b). It can be seen that the synchronization is recovered within four fires after the new oscillator is added.

VI. CONCLUSION

The present paper has investigated the dynamics of globally pulse-coupled oscillators with a refractory period and frequency distribution. Furthermore, on the basis of the stability analysis for the synchronization, the problem concerning how to design oscillators so that they synchronize within a desired number of fires for any initial condition and disturbance has been solved. These analytical results were verified by numerical simulations.

APPENDIX: DISCRETE-TIME MAP OF THE NETWORK

The dynamics of the network described by (1), (2), (3), (4) can be described by a discrete-time nonlinear map. Let the phase of i-th oscillator at time t^{k+} and $t^{(k+1)+}$ be $\phi_i(k) := \phi_i\left(t^{k+}\right)$ and $\phi_i(k+1) := \phi_i\left(t^{(k+1)+}\right)$, then the map from $\phi_i(k)$ to $\phi_i(k+1)$ is given by

$$\phi_i(k+1) = \begin{cases} h_i\left(\phi_i(k)\right) & \text{if } h_i\left(\phi_i(k)\right) < \delta \\ 0 & \text{otherwise} \end{cases},$$

$$h_i\left(\phi_i\right) := \phi_i + \omega_i \min_{j \in \{0,1,\ldots,N-1\}} \frac{1-\phi_j}{\omega_j}.$$

This discrete-time map is helpful to simulate the dynamics of the network.

---

[1] T. Endo and S. Mori. Mode analysis of a multimode ladder oscillator. *IEEE Trans. Circuits and Systmes*, 23:100–113, 1976.

[2] T. Endo and S. Mori. Mode analysis of a ring of a large number of mutually coupled van der pol oscillators. *IEEE Trans. Circuits and Systmes*, 25:7–18, 1978.

[3] Y. Nishio and A. Ushida. Spatio-temporal chaos in simple coupled chaotic circuits. *IEEE Trans. Circuits and Systmes-I*, 42:678–686, 1995.

[4] K. Kaneko. *Theory and applications of coupled map lattices*. Wiley, Chichester, England, 1993.

[5] A. Pikovsky, M. Rosenblum, and J. Kurths. *Synchronization*. Cambridge University Press, 2001.

[6] R.E. Mirollo and S.H. Strogatz. Synchronization of pulse-coupled biological oscillators. *SIAM Journal on Applied Mathematics*, 50:1645–1662, 1990.

[7] M. Tsodyks, I. Mitkov, and H. Sompolinsky. Pattern of synchrony in inhomogeneous networks of oscillators with pulse interactions. *Phys. Rev. Lett.*, 71:1280–1283, 1993.

[8] S. Bottani. Pulse-coupled relaxation oscillators: from biological synchronization to self-organized criticality. *Phys. Rev. Lett.*, 74:4189–4192, 1995.

[9] C.C. Chen. Threshold effects on synchronization of pulse-coupled oscillators. *Phys. Rev. E*, 49:2668–2672, 1994.

[10] V. Kirk and E. Stone. Effect of a refractory period on the entrainment of pulse-coupled integrate-and-fire oscillators. *Phys. Lett. A*, 232:70–76, 1997.

[11] W. Gerstner. Rapid phase locking in systems of pulse-coupled oscillators with delays. *Phys. Rev. Lett.*, 76:1755–1758, 1996.

[12] M. Timme, F. Wolf, and T. Geisel. Coexistence of regular and irregular dynamics in complex networks of pulse-coupled oscillators. *Phys. Rev. Lett.*, 89:258701, 2002.

[13] P. Gong and C. vanLeeuwen. Dynamically maintained spike timing sequences in networks of pulse-coupled oscillators with delays. *Phys. Rev. Lett.*, 98:048104, 2007.

[14] W. Wu and T. Chen. Desynchronization of pulse-coupled oscillators with delayed excitatory coupling. *Nonlinearity*, 20:789–808, 2007.

[15] A. Diaz-Guilera, C.J. Perez, and A. Arenas. Mechanisms of synchronization and pattern formation in a lattice of pulse-coupled oscillators. *Phys. Rev. E*, 57:3820–3828, 1998.

[16] P. Goel and B. Ermentrout. Synchrony, stability, and firing patterns in pulse-coupled oscillators. *Physica D*, 163:191–216, 2002.

[17] P. Ostborn. Phase transition to frequency entrainment in a long chain of pulse-coupled oscillators. *Phys. Rev. E*, 66:016105, 2002.

[18] X. Guardiola, A. Diaz-Guilera, M. Llas, and C.J. Perez. Synchronization, diversity, and topology of networks of integrate and fire oscillators. *Phys. Rev. E*, 62:5565–5570, 2000.

[19] W. Garver and F. Moss. Electronic fireflies. *Scientific American*, 269:128–130, 1993.

[20] T. Kousaka, H. Kawakami, and T. Ueta. Synchronization of electric fireflies by using square wave generators. *IEICE Trans. Fundamentals*, E81-A:656–663, 1998.

[21] G.M.R. Ávila, J.L. Guisset, and J.L. Deneubourg. Synchronization in light-controlled oscillators. *Physica D*, 182:254–273, 2003.

[22] G.M.R. Ávila, J.L. Guisset, and J.L. Deneubourg. Synchronization in chains of light-controlled oscillators. *Journal of Physics: Conference Series*, 23:252–258, 2005.

[23] H. Nakano, T. Saito, and K. Mitsubori. Synchronization from pulse-coupled integrate-and-fire chaotic oscillators. *IEICE Trans. Fundamentals*, E83-A:895–900, 2000.

[24] H. Nakano and T. Saito. Grouping synchronization in a pulse-coupled network of chaotic spiking oscillators. *IEEE Trans. Circuits and Sys. I*, 15:1018–1026, 2004.

[25] J.M. Kahn, R.H. Katz, and K.S.J. Pister. Mobile networking for smart dust. *ACM/IEEE Intl. Conf. on Mobile Computing and Networking*, pages 271–278, 1999.

[26] F. Sivrikaya and B. Yener. Time synchronization in sensor networks: a survey. *IEEE Network*, 18:45–50, 2004.

[27] D. Lucarelli and I.J. Wang. Decentralized synchronization protocols with nearest neighbor communication. *Proc. of SenSys'04*, 62–68, 2004.

[28] G. Werner-Allen, G. Tewari, A. Patel, M. Welsh, and R. Nagpal. Firefly-inspired sensor network synchronicity with realistic radio effects. *Proc. of SenSys'05*, 142–153, 2005.

[29] N. Wakamiya and M. Murata. Synchronization-based data gathering scheme for sensor networks. *IEICE Trans. Commnu.*, E88-B:873–881, 2005.

[30] A.S Hu and S.D. Servetto. On the scalability of cooperative time synchronization in pulse-connected networks. *IEEE Trans. Information Theory*, 52:2725–2748, 2006.

[31] O. Simeone, U. Spagnolini, and Y. Bar-Ness. Small-world effects of shadowing in pulse-coupled distributed time synchronization. *IEEE Communications Letters*, 11:1–3, 2007.

[32] O. Simeone, U. Spagnolini, G. Scutari, and Y. Bar-Ness. Physical-layer distributed synchronization in wireless networks and applications. *Physical Communication*, 1:67–83, 2008.

[33] Y.W. Hong and A. Scaglione. A scalable synchronization protocol for large scale sensor networks and its applications. *IEEE Journal on selected areas in communications*, 23:1085–1099, 2005.